Final Draft
of the original manuscript:

Wischke, C.; Krueger, A.; Roch, T.; Pierce, B.F.; Li, W.; Jung, F.; Lendlein, A..:
Endothelial cell response to (co)polymer nanoparticles depending on the inflammatory environment and comonomer ratio
In: European Journal of Pharmaceutics and Biopharmaceutics (2013) Elsevier

DOI: 10.1016/j.ejpb.2013.01.025

Endothelial cell response to (co)polymer nanoparticles depending on the inflammatory environment and comonomer ratio

Christian Wischke[1,2,3,4], Anne Krüger[1,4], Toralf Roch[1,3], Benjamin F. Pierce[1,2,3], Wenzhong Li[1], Friedrich Jung[1,2,3], Andreas Lendlein[1,2,3]*

[1] Institute of Biomaterial Science, Helmholtz-Zentrum Geesthacht, Kantstr. 55, 14513 Teltow, Germany

[2] Berlin-Brandenburg Centre for Regenerative Therapies, Berlin and Teltow, Germany

[3] Helmholtz Virtual Institute − Multifunctional Materials for Medicine, Teltow and Berlin, Germany

[4] Authors contributed equally

* Corresponding author: A. Lendlein, E-mail address: andreas.lendlein@hzg.de; Tel: +49 (0)3328 352 450; Fax: +49 (0)3328 352 452.

Abstract

Endothelial cells lining the lumen of blood vessels serve as a physiological barrier controlling nanoparticle movement from the vasculature into the tissue. For exploring the effect of polymer hydrophilicity on nanoparticle interactions with human umbilical vein endothelial cells (HUVEC) *in vitro*, a series of monomodal poly[acrylonitrile-*co*-(*N*-vinylpyrrolidone)] model nanoparticles with increasing hydrophilicity as related to their increasing content (0-30 mol.%) of *N*-vinylpyrrolidone (NVP) were synthesized by miniemulsion polymerization. Nanoparticles with a low NVP content were rapidly endocytized into all cells independent from the particle dose with toxic effects only observed at high particle concentrations, while only 10-30% of the cells incorporated particles with ≥ 20 mol.% NVP. Since pathologies are often related to inflammation, an inflammatory HUVEC culture condition with IL-1β stimulation has been introduced and suggested to be widely applied for studying nanocarriers, since cellular uptake in this assay was clearly increased for NVP contents ≥ 20 mol.%. Importantly, the secretion of functional biological mediators by HUVECs was not relevantly influenced by the nanoparticles for both homeostatic and inflammatory conditions. These findings may motivate concepts for nanocarriers specifically targeted to pathologic regions. Additionally, rapidly endocytized Rhodamin B loaded particles with low NVP content may be explored for cell labeling and tracking.

Keywords: Nanoparticle toxicity, human umbilical vein endothelial cells, poly[acrylonitrile-*co*-(*N*-vinylpyrrolidone)], endocytosis, inflammatory cell culture conditions, miniemulsion polymerization

1. Introduction

The fascinating concept of modulating the biodistribution and cellular uptake of particulate carriers by a matrix size reduction has put great expectations into the field of nanoparticle technology. It was indicated that certain nanocarriers may not only penetrate into the skin but may permeate through it for systemic delivery of encapsulated drugs [1]. For nanocarriers injected intravenously, a reduced vascular integrity of tumor tissue due to lesions in-between the endothelial cells led to the theory of enhanced permeation and retention (EPR), by which drug-loaded particles would extravasate and possibly distribute into the tumor tissue for a more effective treatment [2]. In addition to tumor targeting, nanoparticle delivery to specific organs has been focused on by facilitating a reported inherent capability of specific families of biomaterials to overcome intact endothelial layers such as the very effective blood-brain barrier for brain targeting [3]. Despite these remarkable findings, the research community is presently developing a more critical view on the opportunities, challenges, and limitations of nanoparticulate carriers for both topical [4] and intravenous [5] administration. One concern, which has also been recognized by the public, is a potential short- or long-term toxicity of nanoparticles [6]. Therefore, systematic studies remain of high relevance that evaluate cellular fate based on properties of nanoparticles, which may be injected as carrier systems for drug delivery, originate from environmental sources or implant abrasions, or may be employed in bioimaging to label and potentially track cells.

When focusing on an *in vivo* scenario, nanoparticles that have entered the body by one or the other pathway will, upon their distribution in the body through the vascular system, contact endothelial cells (ECs) as the top luminal cell layer in vessels. As applicable for all mammalian

cells, ECs possess the capability for endocytosis, for example, for uptake of nutrients by a number of different pinocytic pathways [7], which may also be followed by nanoparticles entering the cells. Nanoparticle surface functionalization may ideally result in an accumulation in a certain pathologic tissue or in a defined uptake pathway to be followed [8]; the biological consequences of nanoparticle entry into ECs by either one or the other pinocytic pathway are currently not fully understood. Similarly, *in vivo* EC interaction with nanoparticles may strongly differ from standard cell culture conditions in numerous *in vitro* studies. In particular, physiological processes such as blood flow that limits the approximation of particles to the ECs [9] and reduces their uptake [10] as well as pathophysiological conditions such as inflammation are rarely considered [11]. In particular, an inflammatory environment, as can be mimicked *in vitro* by pro-inflammatory cytokines such as IL-1β [12], can be expected not only to alter paracellular transport by modulation of EC tight junctions [13], but it was hypothesized to also affect the EC endocytic activity and/or response to engulfed nanoparticles.

In addition to the assumed response of EC functionality to inflammation, different nanoparticle properties such as the hydrophobicity of the polymer matrix as related to the polymer composition are believed to be important contributors to their interaction with cells either directly or indirectly as mediated by adsorbed proteins [14]. In order to provide model materials with systematic variation of hydrophilicity, a suitable copolymer system with increasing capacities to interact with water may be a rational approach. Copolymers from monomers substituted with side chains of different hydrophobicity such as poly(alkyl-2-cyanoacrylates) [15] or poly(alkyl methacrylate) [16] are examples of polymer systems with tunable properties, but possible contributions of the dangling side chains in the interaction with cells may be difficult to evaluate. Alternatively, comonomers forming repeating units of different

hydrophilicities that do not carry spacious side chains may be copolymerized. Here, based on the reported hemo- and biocompatibility of membranes from acrylonitrile (AN)-based (co)polymers [17], poly[acrylonitrile-*co*-(*N*-vinylpyrrolidone)]s [P(AN-*co*-NVP)] were selected for this study as a family of materials, in which an increasing molar content of *N*-vinylpyrrolidone (NVP) correlates with an increasing material hydrophilicity and water uptake.

In order to systematically study the interaction of P(AN-*co*-NVP)-based nanoparticles with ECs, monomodal, narrow particle size distributions were envisioned, which ideally should be formed by combining copolymer synthesis and particle formation in an integrated process. The synthesis of AN-based nanoparticles has been systematically studied, mostly based on (macro)emulsion/dispersion polymerization [18-20], which in some cases involved the use of solvents or metal based catalysts with assumed toxicity and/or may result in particles with a larger size distribution. Several of these challenges can be overcome by acrylonitrile copolymerization in miniemulsions [21], in which less surfactant is required when compared to the high detergent levels used for polyacrylonitrile nanoparticle synthesis in microemulsions [22] and a hydrophobic costabilizer impedes Ostwald ripening of nascent droplets/particles, thereby enabling narrow size distributions.

In the present study, a series of copolymer nanoparticles from P(AN-*co*-NVP) with low cytotoxicity for a murine fibroblast cell line [23] have been synthesized in a miniemulsion process and doped with Rhodamin B dye to enable visualization and quantification of their interaction with primary human umbilical vein endothelial cells (HUVECs). Importantly, besides a detailed characterization of nanoparticle composition and morphology, the response of HUVECs to nanoparticle exposure was analyzed not only under standard cell culture conditions,

but additionally also in an inflammatory environment, thus mimicking conditions possibly present under pathologic conditions.

2. Materials and methods

2.1. Materials

The comonomers acrylonitrile (AN; ≥ 99.0%, distilled at 77 °C prior to use) and 1-vinyl-2-pyrrolidone (NVP; ≥ 99%, purified on syringe column packed with inhibitor removers) as well as the initiator 2,2'-azobis-(2-methyl-butyronitrile) [AMBN; ≥ 98.0%], the stabilizer sodium dodecyl sulfate (SDS; ≥ 99.0%), the dye Rhodamin B, and the solvent hexadecane (≥99.8%; Fluka brand) were purchased from Sigma-Aldrich (Steinheim, Germany). All other chemicals were of analytical grade.

2.2. Synthesis of nanoparticles

In order to achieve highest purity of nanoparticles, the synthesis based on an oil-in-water (o/w) emulsion and the subsequent purification was performed with depyrogenized glassware in a biological safety cabinet under laminar air flow. The continuous w-phase consisted of 38 ml of water substituted with 80 mg of SDS. The o-phase was prepared by first dispersing 0.333 mg Rhodamin B in 200 mg hexadecane and adding a total of 2 g of AN/NVP monomers with different molar ratios. After pre-emulsification by magnetic stirring at 650 rpm in a pressure tube (100 ml, 17.8 cm length × 38.1 mm O.D.) for 1 h, 40 mg of AMBN was added and the mixture was sonicated for 4 min in an ice bath for nanodispersion of the o-phase droplets (Sonopuls HD 2017 with a 70 G probe, amplitude 90%; Bandelin, Berlin, Germany). The reaction was continued at 77 °C in closed vessels under magnetic steering at 600 rpm for 7 h. Purification by

dialysis was performed with diluted aliquots (25 ml + 65 ml sterilized water) in ethylene oxide-sterilized dialysis tubing (Visking type 20/32, MWCO 14,000 Da cutoff; Carl Roth, Karlsruhe, Germany) for 6 d at room temperatures with frequently replaced 2.5 ml sterilized water as external medium. Rhodamin B did leak neither during dialysis nor during release experiments at 37 °C into the medium as analyzed by HPLC. Depending on the percent relative molar feeding ratio R of NVP with $R = n_{NVP} \cdot (n_{NVP} + n_{AN})^{-1}$, the copolymer nanoparticles were denoted as P(AN-*co*-NVP) R, for example, P(AN-*co*-NVP) 10 as prepared by using 1.654 g AN and 0.346 g NVP monomers during synthesis.

2.3. Chemical composition of nanoparticles

The composition of nanoparticles as obtained after synthesis was characterized by ^{1}H NMR on a 500 MHz Bruker Avance spectrometer (Karlsruhe, Germany) in dimethyl sulfoxide-d6 (Sigma Aldrich, Steinheim, Germany). ^{1}H-NMR (500 MHz, DMSO-d6) δ (ppm) = 4.38-4.18 (1H, d), 3.38-3.29 (2H, g), 3.25-2.98 (1H, b), 2.92-2.60 (2H, e), and 2.35-1.70 (6H, f + a + c). Additionally, elemental analysis (EA) was performed with a vario EL III (Elementar, Hanau, Germany) with a thermal conductivity detector in a helium atmosphere.

2.4. Particle size, charge, and morphology

Particle sizes were determined by dynamic light scattering on a Delsa™Nano C (Beckman Coulter, Krefeld, Germany) with dilution of 50–100 µl of the nanoparticle samples in 1 ml water. Measurements were performed at 20 °C in quartz glass cuvettes and scattering pattern analyzed at an angle of 165° with the Contin model.

Particle size and morphology were additionally evaluated by scanning electron microscopy (SEM) on a Gemini SupraTM 40 VP (Carl Zeiss NTS, Oberkochen, Germany) at 10 kV with a secondary electron detector. Sample preparation involved their spreading on a silicon waver using a spin coater at 5000 rpm (Laurell Spin Coater Modell 650) and their sputtering with iridium.

Analysis of particle powders by Wide-Angle X-ray Scattering (WAXS) was performed at room temperature on a D8 Discovery (Bruker, Karlsruhe, Germany).

2.5. Cultivation of human umbilical vein endothelial cells

Endothelial cells were cultured from human umbilical vein (HUVEC, Lonza, Cologne, Germany) in endothelial basal medium (EBM-2, Lonza) supplemented with EGM-2 SingleQuots® (Lonza) at 37 °C and 5% CO_2 in polystyrene-based cell culture flasks (TPP, Trasadingen, Switzerland). For biological experiments, cells were cultivated until passage 4, trypsinized, and seeded with 4400 cells/well in polystyrene 96-well plates (Corning®, NY, USA) for titration experiments and subsequently with 25,000 cells/well in polystyrene 24-well plates (Greiner Bio-One, Frickenhausen, Germany). Inflammatory conditions in HUVECs culture were induced using human recombinant IL-1β (10 ng ml^{-1}), which was added to HUVECs after cell seeding. As a control, HUVEC cultivated without nanoparticles were used. Additionally, in controls with soluble Rhodamin B, no alteration of the cell status was detected (data not shown).

2.6. Nanoparticle uptake, toxicity, and endotoxin quantification

Nanoparticle uptake frequencies were analyzed by flow cytometry using the MACSQuant® analyzer (Miltenyi Biotec) after trypsinization and the signal was provided by Rhodamin B dye

loaded in the nanoparticles. To discriminate live and dead cells, 1 $\mu g \cdot ml^{-1}$ 4',6-diamidino-2-phenylindole (DAPI) was added immediately prior to analysis, while cells were kept at 4 °C to minimize metabolic activity and active uptake pathways of living cells and to selectively stain dead cells. Additionally, cytotoxicity testing was performed by analyzing the membrane integrity based on the levels of released lactate dehydrogenase (LDH assay; Cytotoxicity Detection Kit, Roche, Grenzach, Germany) and the metabolic activity of HUVECs by conversion of 3-(4,5-dimethylthiazol-2-yl)-5-(3-carboxymethoxyphenyl)-2-(4-sulfophenyl)-2H-tetrazolium (MTS assay) to a colored formazan product by intracellular reductases (CellTiter 96® AQueous Non-Radioactive Cell Proliferation Assay, Promega, Mannheim, Germany) incubated with nanoparticles (60 $\mu g/10^5$ cells) for 24 h and 72 h. To induce cell dead as positive control for LDH and MTS assay, Triton-X 0.5% dissolved in PBS and $CuCl_2$ solution (1mmol l^{-1}), respectively, was used.

For the analysis of lipopolysaccharide (LPS) contaminations, eluates of the nanoparticles were prepared by a downscaled DIN ISO 10993–12 method with incubation of 30 mg nanoparticles in Minimum Essential Medium (MEM) for 72 h and subsequent characterization by the chromogenic Limulus amoebocyte lysate (LAL) assay (Lonza, Cologne, Germany).

2.7. Profiles of soluble factor secretion of HUVECs

Supernatants from cell culture were collected after 72 h (60 µg nanoparticles/10^5 cells). The prostacyclin (PGI_2) and thromboxane A_2 (TXA_2) secretion by HUVECs were analyzed using competitive-enzyme immunoassays detecting hydrolyzed 6-keto Prostaglandin $F_{1a\alpha}$ as a PGI_2

metabolite and thromboxane B_2 as a TXA_2 metabolite (6-keto-Prostaglandin $F_{1\alpha}$ EIA Kit and Thromboxane B_2 EIA Kit, Cayman Chemical Company, Ann Arbor; MI, USA). To investigate the secretion of cytokines such as IL-1ra, bFGF, PDGF-BB, IL-6, TNF-α, and VEGF by HUVECs, the Multiplex technique (Bio-Plex200®, BioRad Laboratories Munich, Germany) was used. The matrix metalloprotease (MMP) activity was determined using the pan-MMP fluorogenic peptide substrate Mca-PLGL-Dpa-AR-NH2 (R&D Systems). Recombinant human MMP-9 (R&D Systems) served as the positive control (25 $ng \cdot ml^{-1}$).

2.8. Immunocytochemistry

In order to visualize both extracellular matrix components and the localization of nanoparticles inside the cells, HUVECs were fixed in paraformaldehyde (4 wt.%; 30 min, on ice) after 72 h of nanoparticle incubation. Subsequently, cells were permeabilized with Triton-X100 in water (0.5% w/v) and blocked with a 5% (w/v) solution of bovine serum albumin. Fibronectin was stained with polyclonal sheep anti-human fibronectin antibody (R&D Systems GmbH, Wiesbaden-Nordenstadt, Germany) and donkey anti-sheep DyLight 488 (Jackson Immuno Research, Laboratories, Inc., Suffolk, UK). Nuclei were labeled with DAPI (Roth, Karlsruhe, Germany). Samples were analyzed using confocal laser scanning microscopy (LSM 510 META, Zeiss, Jena, Germany) with 100x primary magnification.

2.9. Statistical analysis

The results of the cell studies were confirmed in a minimum of two independent experiments. Data were statistically analyzed by GraphPad Prism (La Jolla, CA, USA), and the median and range were calculated.

3. Results and discussion

3.1. Copolymer nanoparticles with increasing content of hydrophilic N-vinylpyrrolidone

Poly[acrylonitrile-*co*-(*N*-vinylpyrrolidone)] nanoparticles were prepared in an integrated process of copolymer synthesis and particle formation using a miniemulsion based approach [23]. This involved the use of hexadecane as a hydrophobic costabilizer in addition to SDS [21] to stabilize the o/w emulsion of the mixed comonomers AN and NVP. Based on the preferred solubility of the selected initiator AMBN in hydrophobic environments, radical polymerization can be expected to occur preferentially in the oil-phase [24,25] with the fraction of monomers that have been dissolved in water continuously diffusing to the nascent particles for finally being incorporated in the growing polymer chains. Importantly, in order to allow for highest purity of samples without immunogenic impurities, all process steps including synthesis and subsequent purification by dialysis were performed with depyrogenized glassware and sterilized aqueous media in a biological safety cabinet under laminar air flow. Rhodamin B was loaded into the particles as a dye that would later enable the quantitative evaluation of their potential endocytosis by endothelial cells. Neither during dialysis of the synthesized particles at room temperature nor during incubation of particles dispersed in aqueous media at 37 °C could any leakage of Rhodamin B to the medium be detected by HPLC.

The ^{1}H NMR evaluation of the copolymer composition revealed some deviations of the determined NVP content from the relative NVP molar feeding ratio *R* during synthesis (Table 1). The higher reactivity of NVP monomers under most experimental conditions [26] may explain its disproportionally high incorporation into the copolymer at low *R*, while at high *R* additional effects such as the distribution between the water- and oil-phase may have reduced its incorporation. The presence of only one mixed rather than separated glass transitions with systematically increasing, composition dependent glass transition temperatures T_g (Table 1) might indicate that copolymers with a random sequence structure rather than block copolymers were formed. While water contact angles of P(AN-*co*-NVP) are known not to depend on the NVP content, there is strong evidence from the literature that increasing NVP contents increase the material hydrophilicity as correlated with both increased water permeation rates and overall equilibrium water uptake [17,27]. Considering the difficult handling of the nanoparticles and the efficient removal of excess stabilizer and non-reacted monomers, the limited nanoparticle yield of typically 50–60 wt.% can be explained. The obtained particle sizes were generally below 200 nm with very narrow size distributions (Table 1), suggesting that the stabilization concept of the miniemulsion was also efficient in the presence of the Rhodamin B dye.

Table 1: Composition and physicochemical properties of nanoparticles with increasing NVP content.

Sample code	*R* (mol.%)	NVP content[a] (mol.%)	Particle yield (wt.%)	T_g (°C)	Crystallinity of particles[b] %	Particle size[c] (nm)	Endotoxin content [I.U.]
p(AN-*co*-NVP) 0	0	0	48	91	31.5±3.8	189±59	<0.06
p(AN-*co*-NVP) 5	5	11	53	119	15.4±2.6	170±49	<0.06

p(AN-*co*-NVP) 10	10	13	61	123	9.5±2.2	171±70	<0.06
p(AN-*co*-NVP) 20	20	21	55	132	0	154±53	<0.06
p(AN-*co*-NVP) 25	25	24	59	137	0	155±44	<0.06
p(AN-*co*-NVP) 30	30	25	58	142	0	139±40	<0.06

[a] Determined by ^{1}H-NMR; [b] Overall relative crystallinity of (co)polymer nanoparticles from WAXS analysis (plots shown as Suppl. Fig. 1); [c] Given values correspond to the intensity distribution determined by DLS.

The particle sizes obtained from dynamic light scattering analysis could be confirmed by SEM, which involved a sample preparation by spin coating in order to obtain monolayers of nanoparticles for best visibility of their size and morphology. Interestingly, the particle structure changed with increasing NVP content from a rough toward a smoother surface morphology (Fig. 1). "Crumpled" structures of polyacrylonitrile homopolymer nanoparticles have been previously reported [21, 18]. Despite no melting transition being observed in DSC curves, WAXS analysis confirmed the presence of crystallites in the studied nanoparticles (Table 1, Suppl. Fig. 1). Thus, it can be expected according to the reference [18] that the rough structure of polyacrylonitrile nanoparticles was derived from crystalline domains within the particles and at their surface, which can be formed due to strong dipole interactions established in the homopolymer. When randomly introducing increasing concentrations of NVP into the polymer chains, the average segment length containing only AN and thus the capability of the copolymer for crystallization will be reduced. Accordingly, the P(AN-*co*-NVP) nanoparticle structures changed toward smoother surfaces with increasing *R* value (Fig. 1), which is in good agreement with transmission electron microscopy (TEM) data for copolymer nanoparticles from AN with another comonomer, styrene [21].

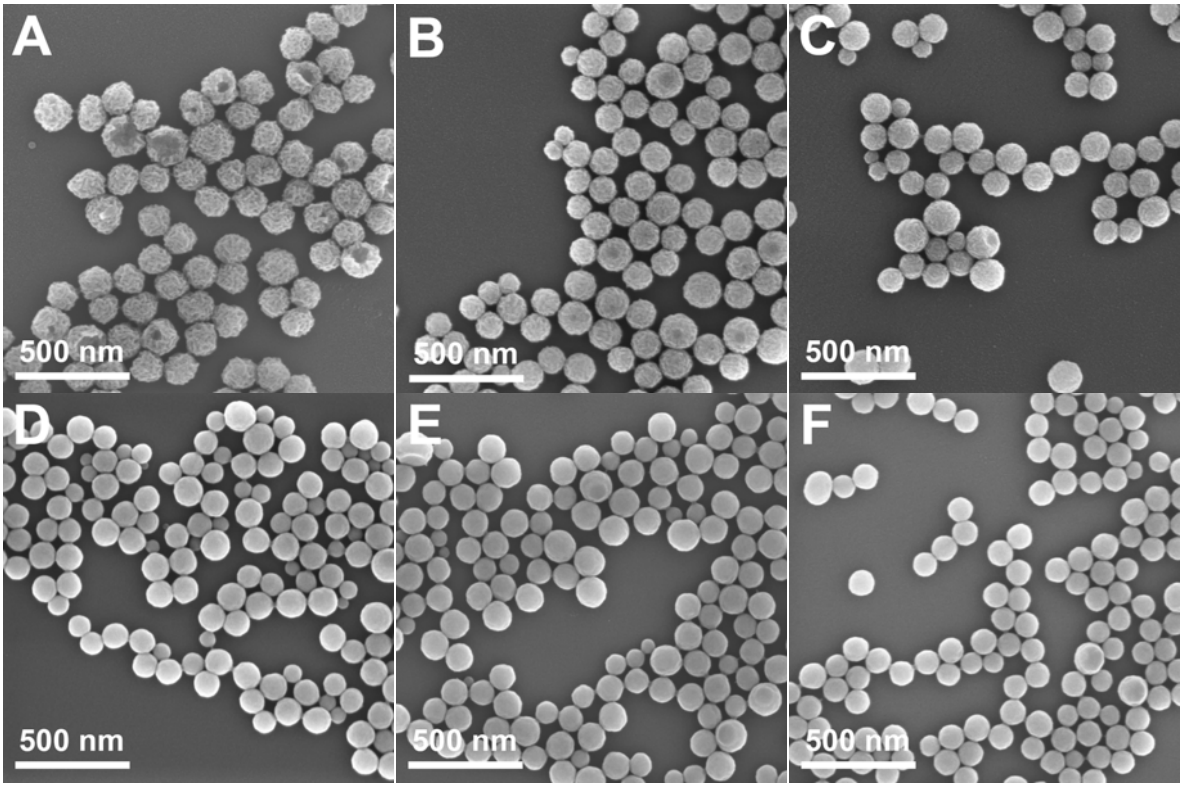

Fig. 1: SEM images of (A) P(AN-*co*-NVP) 0, (B) P(AN-*co*-NVP) 5, (C) P(AN-*co*-NVP) 10, (D) P(AN-*co*-NVP) 20, (E) P(AN-*co*-NVP) 25, and (F) P(AN-*co*-NVP) 30.

3.2. Influence of nanoparticle concentration and composition on HUVECs

For studying the interaction of nanoparticles with HUVECs, a nanoparticle concentration range should first be identified that does not induce cell toxicity. Generally, the particle dose was normalized to the number of seeded cells in order to allow comparability of experiments requiring different total cell numbers, especially for subsequently reported functional analysis of HUVECs (Section 3.3). As illustrated in Fig. 2A, a systematic decrease in viability after 24 h of incubation was observed for P(AN-*co*-NVP) 0 when the nanoparticle dose was increased from 30 to 800 µg per 10^5 cells. With increasing *R* value, this effect was less pronounced with no

impedance of viability being observed for $R \geq 25$ mol.% even at the highest particle concentration.

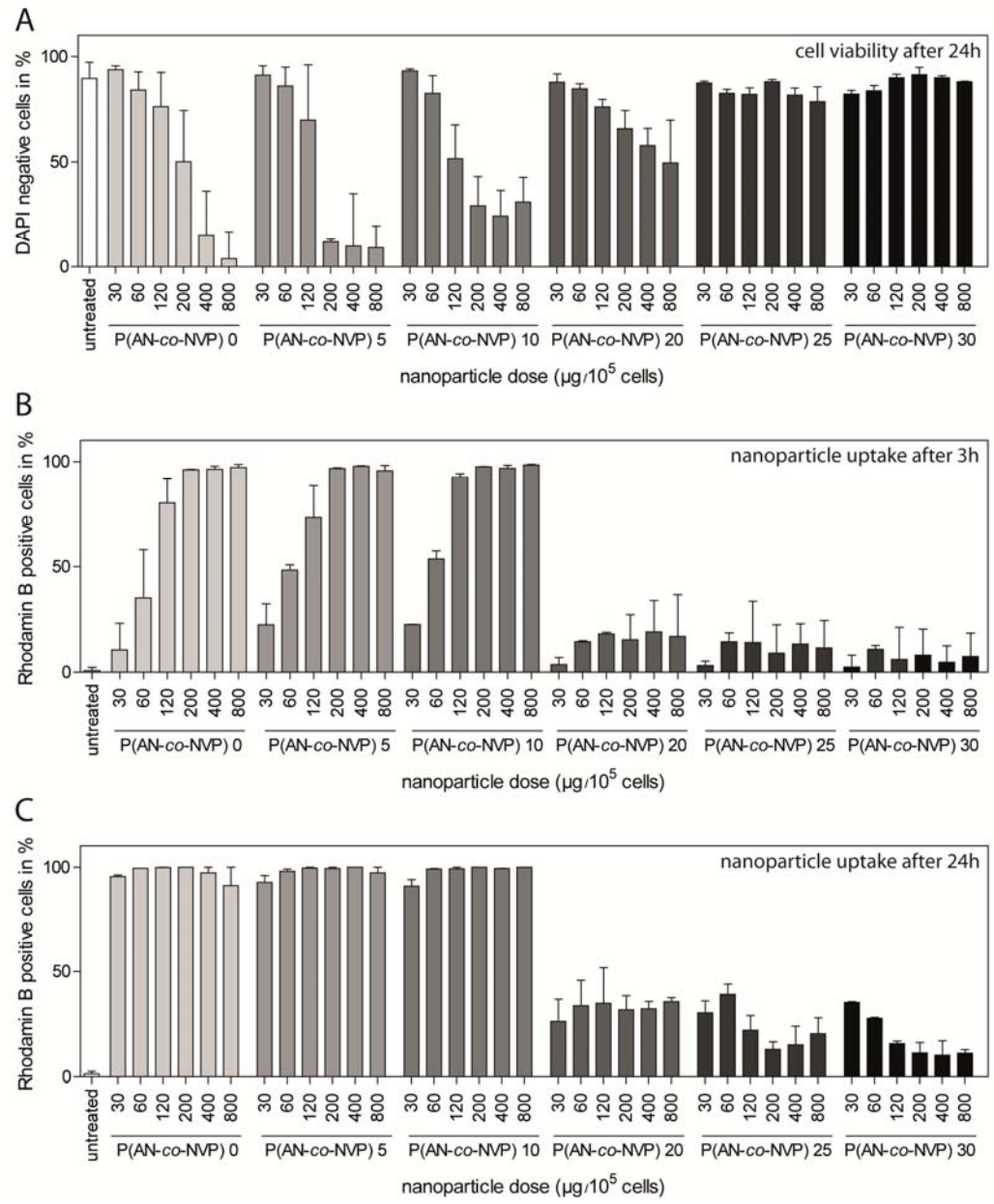

Fig. 2: Flow cytometric analysis of composition- and concentration-dependent effects of P(AN-*co*-NVP) nanoparticles on HUVECs. (A) Cell viability after 24 h of exposure

to nanoparticles as determined by the relative number of DAPI negative cells. (B-C) Uptake of nanoparticles by HUVECs as determined by the fluorescence due to Rhodamin B loaded in the nanoparticles. Data for uptake after 3 h and 24 h of exposure to nanoparticles (n = 3, median, range). The gating strategy is reported as Suppl. Fig. 2.

Based on the previous extensive pretreatment by dialysis, water-soluble leachables could be excluded as having caused the decreasing viability at increasing particle concentrations for *R* values ≤ 10 mol.%. Therefore, a direct interaction of nanoparticles with HUVECs or their uptake by endocytosis was expected to have caused this phenomenon. Confocal microscopy strongly supported the uptake and intracellular localization of the Rhodamin B labeled nanoparticles (Fig. 3), which in the future may be additionally confirmed by TEM studies. It appeared that less nanoparticles were taken up with increasing *R*. In order to proceed from this observation of individual cells to a more quantitative evaluation of numerous cells, the fraction of Rhodamin B positive, thus nanoparticle loaded cells were determined by flow cytometry at different time points of incubation (Fig. 2B and C). At higher particle concentrations, a statistically higher number of interaction events between particles and cells and thus a higher probability of endocytosis were expected. Interestingly, after 3 h of cell exposure to the nanoparticles, a concentration dependent uptake could be detected for *R* values of 0-10 mol.%, while after 24 h, almost every cell contained nanoparticles. In contrast, for higher *R* values of 20–30 mol.%, the equilibrium number of cells with engulfed particles remained below 30%. It appeared that the higher water uptake of the nanoparticles associated with high *R* [17] results in a diminished interaction between HUVECs and P(AN-*co*-NVP) nanoparticles. Cell culture studies

of HUVECs on P(AN-*co*-NVP) films support this finding, since a decrease in HUVEC adhesion to the films, that is, an impaired cell-material interaction, was observed with increasing *R* value.

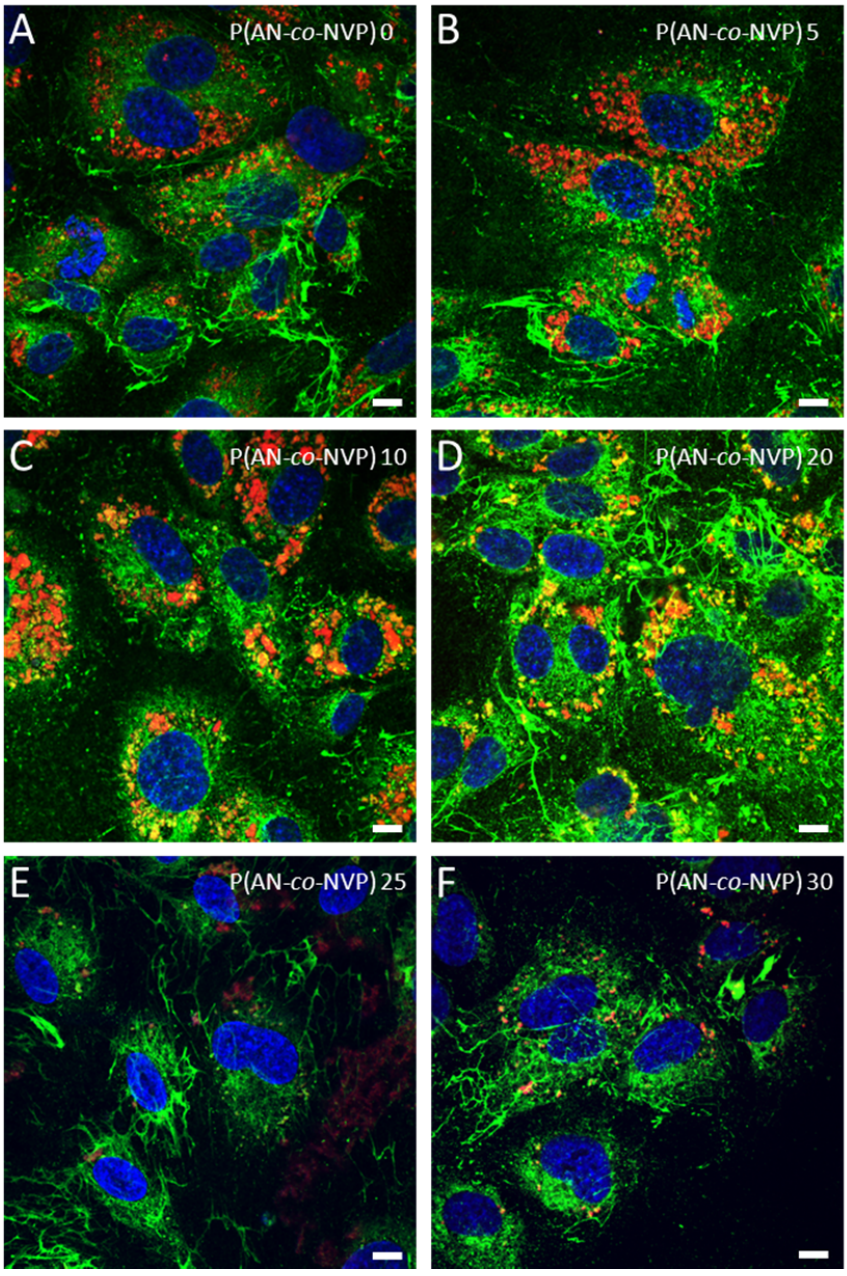

Fig. 3: Confocal microscopic images of cells fixed by paraformaldehyde after 72 h of incubation with 60 µg P(AN-*co*-NVP) nanoparticles per 10^5 cells. Red spots

correspond to aggregates of Rhodamin B labeled nanoparticles, blue to DAPI labeled nuclei, and green structures to fibronectin. Scale bars indicate 10 µm. Controls are reported as Suppl. Fig. 3.

Based on the observed cell viability and efficient uptake at a particle dose of 60 µg per 10^5 cells by flow cytometry (Fig. 2), this condition was selected for subsequent more detailed studies on cell functionalities. The cell viability status was characterized by LDH and MTS assays after 24 h and additionally after 72 h this time interval is relevant for the analysis of soluble factors released by HUVECs. In the LDH assay, which quantifies the release of a cytosolic enzyme through damaged cell membranes, similar LDH levels were identified for particle-treated compared to untreated cells in most cases (Fig. 4A). For some samples, LDH release appeared to be slightly increased, but these values may not be associated with a decreased overall viability as shown by DAPI exclusion in Fig. 2. The increase in mitochondrial enzymatic activity after 72 h compared to 24 h in the MTS assay (Fig. 4B), which similarly occurred for untreated controls and nanoparticle treated cells, could be linked to increasing cell numbers due to HUVEC proliferation. Furthermore, compared to the positive controls of the LDH and MTS tests, the values of the endothelial cell cultures treated with the different nanoparticles composition were completely different, indicating that no substantial cell dead was induced by the particles (Fig. 4A and B).

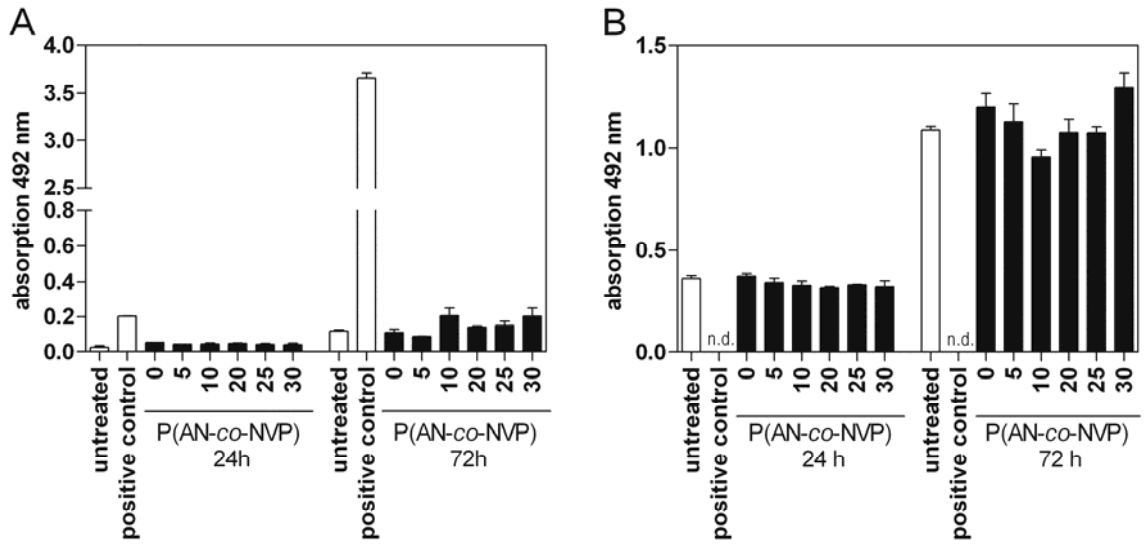

Fig. 4: Analysis of cytotoxic effects of nanoparticles depending on their composition as determined by (A) the LDH test with absorbance correlating with a loss of cell membrane integrity and (B) the MTS test with absorbance correlating with mitochondrial enzymatic activity. All experiments were performed at particles doses of 60 µg per 10^5 cells (n = 2, median, range), n.d. indicates not detectable.

3.3. Response of HUVECs in pro-inflammatory conditions to nanoparticles

Nanoparticles circulating in the blood stream may not exclusively contact endothelial cells with full physiological functionality, but they may also be exposed to areas with pathophysiological conditions, which in some cases may even be the desired target site, as in the case of specific nanoparticulate drug delivery carriers. Inflammation is a complex response of the body to noxious events and is associated with various types of diseases, particularly in their initial phase, which may increase blood vessel permeability by modifying the functional state of endothelial cells as a natural barrier to extravasation. Therefore, inflammatory conditions have been included

in this study as mimicked by addition of IL-1β, which is one of the most potent inflammatory mediators [28] that results in the release of pro-inflammatory mediators such as IL-6 and IL-8 and activation of the NFκB and MAPkinase pathway in endothelial cells [29]. In few cases, confocal microscopy suggested a higher uptake of nanoparticles into HUVECs for the selected non-cytotoxic nanoparticle dose (Fig. 5), at least for the P(AN-*co*-NVP) particles with high *R* that were incorporated only to a minor extent under standard conditions (e.g., compare Figs. 2B and C and 5D).

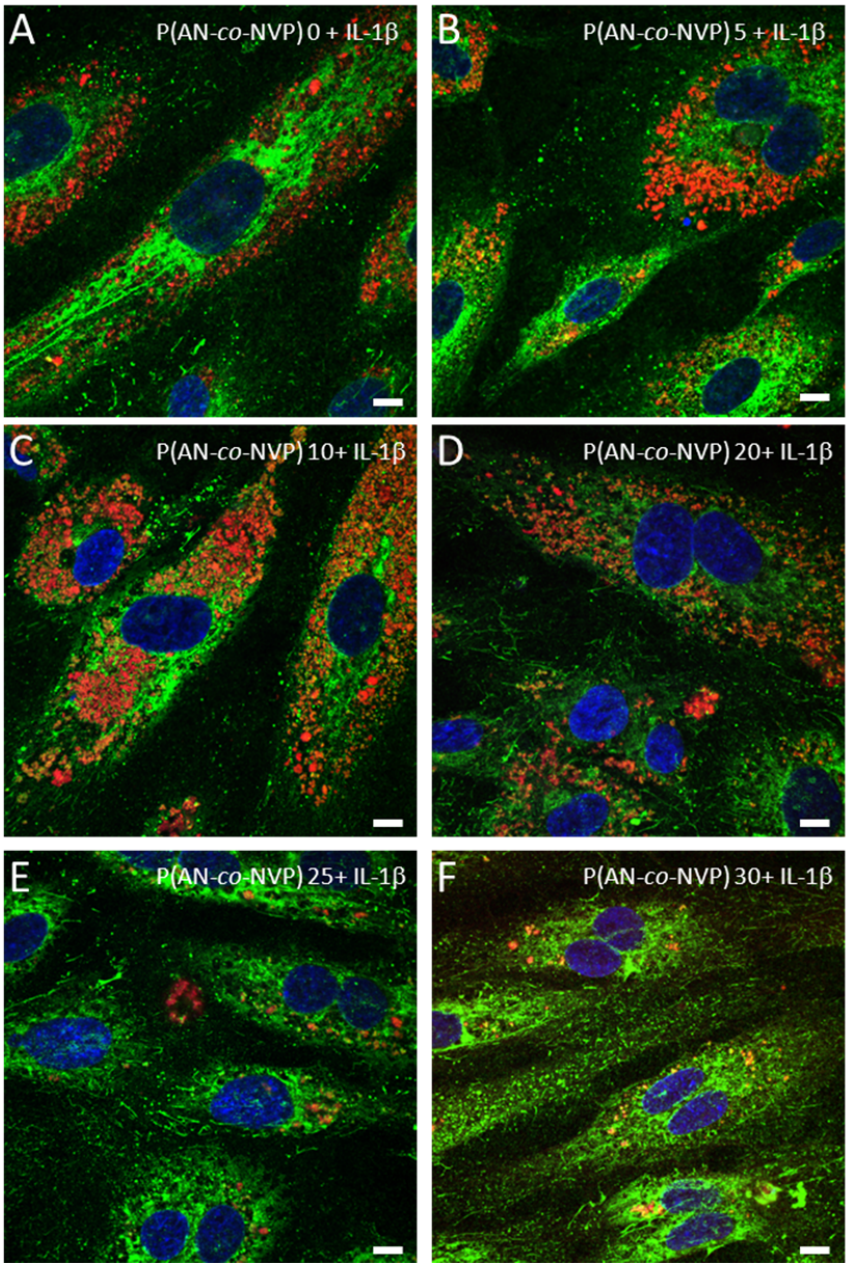

Fig. 5: Confocal microscopic images of cells cultured in the presence of IL-1β (10 ng·ml^{-1}) after 72 h of incubation with 60 µg P(AN-*co*-NVP) nanoparticles per 10^5 cells. Cells were fixed with paraformaldehyde before microscopy. Scale bars indicate 10 µm. For further details see Fig. 3.

In order to confirm and quantify this result as well as to explore its general applicability to various nanoparticle concentrations, the endocytic uptake of P(AN-*co*-NVP) particles with *R* values of 20–30 mol.% was explored by flow cytometry (Fig. 6). The side-by-side comparison in this experiment clearly shows a trend to an increased capability of HUVECs for nanoparticle uptake under inflammatory conditions for the entire tested range of different particle concentrations and compositions. This was obviously relevant only for those copolymer compositions that poorly interacted with HUVECs under standard conditions. The relative increase in uptake under IL-1β conditions was in the range of 30-50% for these samples. These data suggest that a preferential uptake into endothelial cells of pathologic vessel regions may be achieved for suitable nanoparticle compositions, which possibly could be taken advantage of as a targeting strategy in drug delivery.

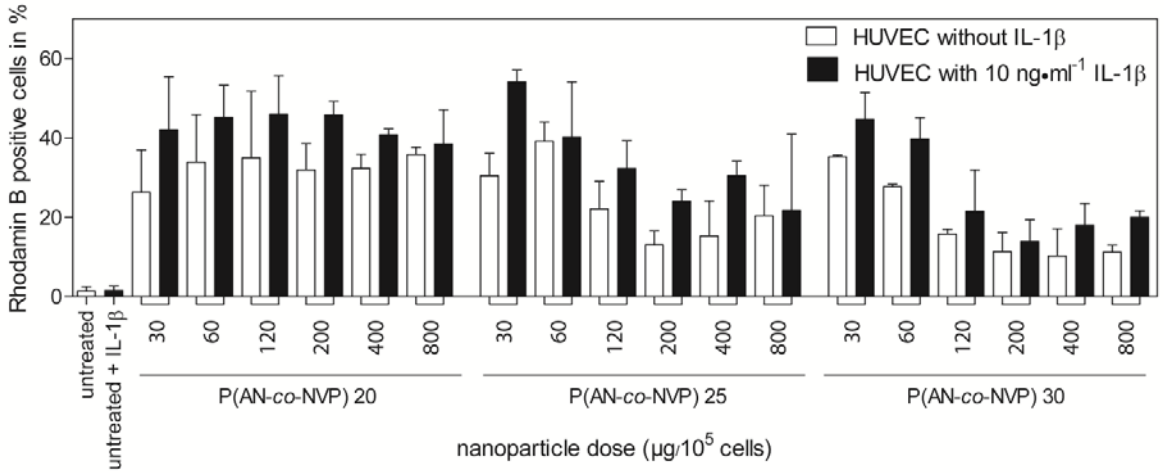

Fig. 6: Enhancement of endocytic uptake of P(AN-*co*-NVP) nanoparticles with high *R* values in inflammatory environment (n = 3, median, range).

3.4. Functional response of HUVECs to P(AN-co-NVP)

By analyzing the cell viability status, the induction of cell death by nanoparticle uptake could be excluded at the selected nanoparticle dose (Fig. 4). In the next step, the release of enzymes and/or signaling molecules, such as stimulatory mediators as relevant for endothelial cell interactions with other cells/blood components, should be characterized since this is a more sensitive tool to evaluate alterations in cell functionality. As shown in Fig. 7, the quantified concentrations of soluble factors were similar to the respective controls for both hemostatic as well as inflammatory condition in most cases. While the employed MMP standard resulted in high fluorescence intensity created by cleavage of a fluorogenic substrate, no elevated levels of secreted MMP were observed in any case for the nanoparticle treated cells (Fig. 7A). For the data interpretation of the subsequently analyzed secretion of inflammatory molecules such as IL-6 it should be considered, that a cytokine release may be a cellular response to the polymeric matrix of the nanoparticles or to immunogenic impurities possibly associated to the particles. Therefore, a careful preparation process of nanoparticle synthesis with sterilized materials in a safety cabinet was applied to prevent contaminations. The analysis of endotoxins by the LAL test confirmed that a non-detectable and thus likely insignificant endotoxin burden could be realized by this procedure (Table 1). While in some cases the IL-6 secretion was diminished compared to the untreated control, this may not be interpreted as an anti-inflammatory effect as it was likely not of biological relevance when considering the extremely high levels of IL-6 secreted in an inflammatory (IL-1β induced) environment (Fig. 7B). In the case of PDGF as a proangiogenic substance, an apparently systematic correlation of factor release and material composition was observed, which so far could not be linked to a specific cellular mechanism (Fig. 7C). For TXA_2 as a prothrombogenic and vasoconstrictive factor as well as PGI_2 as an antithrombogenic

vasodilatative factor (Fig. 7D and E), the unchanged levels of each of the two opponent molecules for all compositions suggested a well preserved balance of this sensitive system that *in vivo* regulates, for example, platelet activation and aggregation. The increased ratio of PGI_2 and TXA_2 secretion for the IL-1β condition confirmed that HUVECs could react also in the presence of nanoparticles to the inflammatory environment, since relative upregulation of PGI_2 is one of the main strategies to increase vessel permeability and allow immune cells to enter the adjacent tissue. Overall, when also considering the unaltered secretion of other tested factors such as VEGF, TNF-α, bFGF, or IL-1ra (data not shown), these results suggest that the functional state of HUVECs was not or, in selected cases, only slightly effected by the different P(AN-*co*-NVP) nanoparticle composition at the studied intermediate particle concentration.

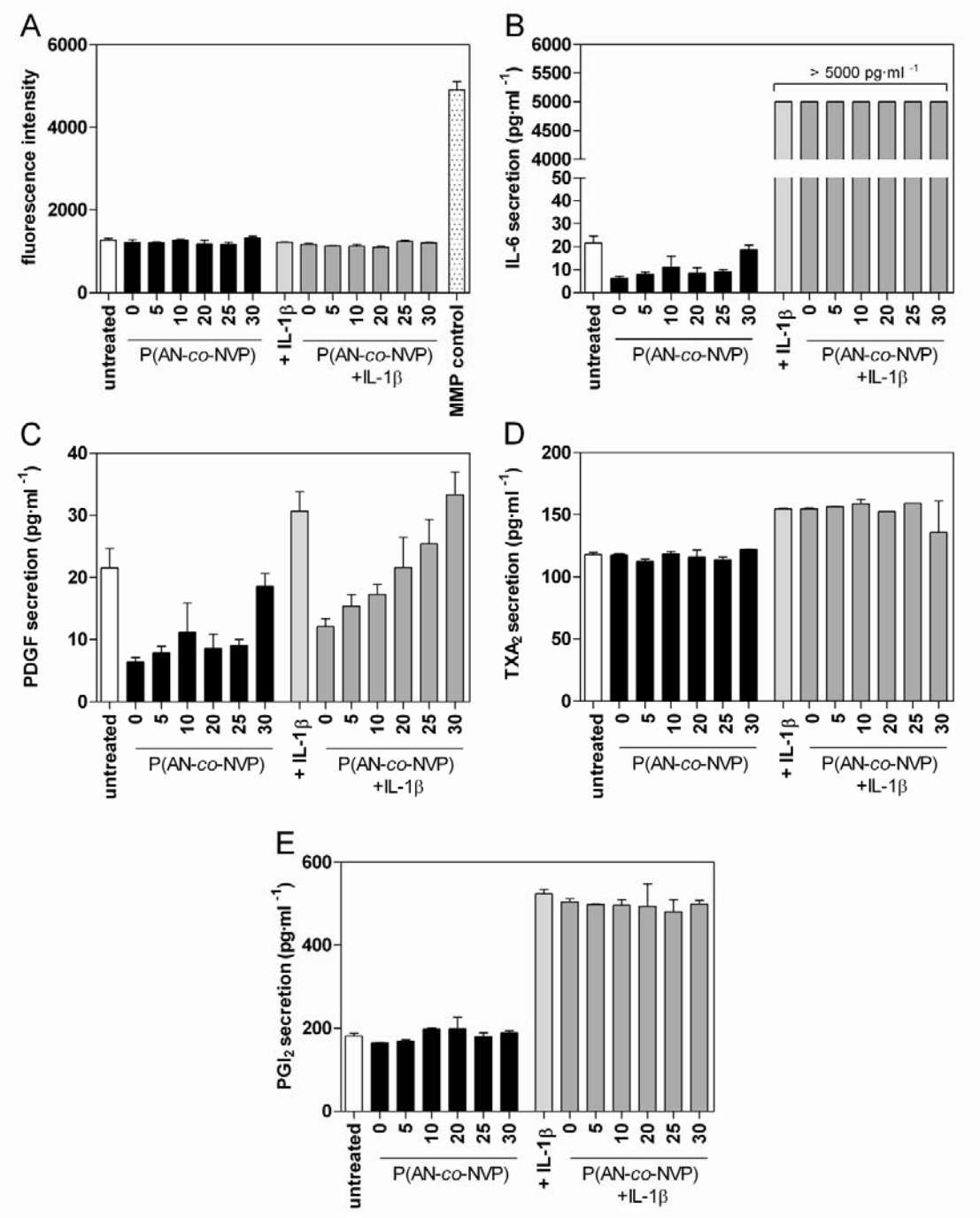

Fig. 7: Secretion of (A) MMP, (B) IL-6, (C) PDGF, (D) TXA_2, and (E) PGI_2 as functional biological mediators by HUVECs depending on nanoparticle composition and

inflammatory environment mimicked by addition of 10 ng·ml^{-1} IL-1β. (n = 2, median, range)

4. Conclusions

A series of model nanoparticles for systematic studies of cell-particle interaction have been successfully prepared from poly[acrylonitrile-*co*-(*N*-vinylpyrrolidone)] by miniemulsion polymerization, resulting in particles with a diameter <200 nm, a narrow size distribution, and varying *N*-vinylpyrrolidone contents. Here, the nanoparticle interaction with endothelial cells is explored, since these cells form the barrier layer that nanoparticles face upon their distribution in the body through the vascular system. Strong differences in the endocytic uptake by HUVECs were observed at various particle concentrations depending on the nanoparticle composition and the cellular environment, namely, the absence or presence of inflammatory conditions. Importantly, the uptake of the nanoparticles up to intermediate concentrations did not affect the viability and functionality of the HUVECs.

While the focus of this study was to systematically investigate the interaction of a series of P(AN-*co*-NVP)-based model nanoparticles with HUVECs under variation of the polymer's hydrophilicity, the observed rapid engulfment of nanoparticles with low *N*-vinylpyrrolidone content in almost all cells at non-cytotoxic concentrations may motivate further exploration of dye loaded particles of these compositions for cell labeling and tracking. On the other hand, the enhancement of uptake of P(AN-*co*-NVP) nanoparticles with high *N*-vinylpyrrolidone content in endothelial cells exposed to an inflammatory environment might be a concept to be followed and translated also into other material systems for an intravascular drug delivery targeted to

pathologic regions. Overall, inflammatory test conditions should be generally included in *in vitro* cell studies of nanotoxicity and nanocarriers.

Acknowledgments

The authors acknowledge the technical support in different parts of this work by Andrea Pfeiffer, Daniela Radzik, Christopher Hortig, Jessica Reinert, Susanne Reinhold, Angelika Ritschel, and Judith Küchler. Partial funding was provided by the German Federal Ministry of Education and Research (grant No. 0315696A Poly4Bio BB).

References

[1] G. Cevc, Drug delivery across the skin, Expert Opin Investig Drugs, 6 (1997) 1887-1937.
[2] K. Iwai, H. Maeda, T. Konno, Use of Oily Contrast-Medium for Selective Drug Targeting to Tumor - Enhanced Therapeutic Effect and X-Ray Image, Cancer Res, 44 (1984) 2115-2121.
[3] B. Petri, A. Bootz, A. Khalansky, T. Hekmatara, R. Muller, R. Uhl, J. Kreuter, S. Gelperina, Chemotherapy of brain turnour using doxorubicin bound to surfactant-coated poly(butyl cyanoacrylate) nanoparticles: Revisiting the role of surfactants, J Control Release, 117 (2007) 51-58.
[4] K. Park, No penetration of nanoparticles through intact skin, J Control Release, 162 (2012) 258-258.
[5] C.J. Cheng, W.M. Saltzman, Downsizing tumour therapeutics, Nat Nanotechnol, 7 (2012) 346-347.
[6] L.M. Bimbo, L. Peltonen, J. Hirvonen, H.A. Santos, Toxicological Profile of Therapeutic Nanodelivery Systems, Current drug metabolism, 13 (2012) 1068-1086.
[7] G. Sahay, D.Y. Alakhova, A.V. Kabanov, Endocytosis of nanomedicines, J Control Release, 145 (2010) 182-195.
[8] S. Muro, C. Garnacho, J.A. Champion, J. Leferovich, C. Gajewski, E.H. Schuchman, S. Mitragotri, V.R. Muzykantov, Control of endothelial targeting and intracellular delivery of therapeutic enzymes by modulating the size and shape of ICAM-1-targeted carriers, Mol Ther, 16 (2008) 1450-1458.
[9] P. Decuzzi, R. Pasqualini, W. Arap, M. Ferrari, Intravascular Delivery of Particulate Systems: Does Geometry Really Matter?, Pharm Res-Dord, 26 (2009) 235-243.
[10] T. Bhowmick, E. Berk, X.M. Cui, V.R. Muzykantov, S. Muro, Effect of flow on endothelial endocytosis of nanocarriers targeted to ICAM-1, J Control Release, 157 (2012) 485-492.
[11] M.I. Hermanns, J. Kasper, P. Dubruel, C. Pohl, C. Uboldi, V. Vermeersch, S. Fuchs, R.E. Unger, C.J. Kirkpatrick, An impaired alveolar-capillary barrier in vitro: effect of proinflammatory cytokines and consequences on nanocarrier interaction, J R Soc Interface, 7 (2010) S41-S54.

[12] M. Pesce, L. Speranza, S. Franceschelli, V. Ialenti, A. Patruno, M.A. Febo, M.A. De Lutiis, M. Felaco, A. Grilli, Biological role of interleukin-1beta in defensive-aggressive behaviour, J Biol Regul Homeost Agents, 25 (2011) 323-329.
[13] W. Qin, W. Lu, H. Li, X. Yuan, B. Li, Q. Zhang, R. Xiu, Melatonin inhibits IL1beta-induced MMP9 expression and activity in human umbilical vein endothelial cells by suppressing NF-kappaB activation, J Endocrinol, 214 (2012) 145-153.
[14] P.P. Karmali, D. Simberg, Interactions of nanoparticles with plasma proteins: implication on clearance and toxicity of drug delivery systems, Expert Opin Drug Del, 8 (2011) 343-357.
[15] C. Wischke, J. Weigel, A.T. Neffe, A. Lendlein, Understanding instability and rupture of poly(alkyl-2-cyanoacrylate) capsules, Int J Artif Organs, 34 (2011) 243-248.
[16] S. Lorenz, C.P. Hauser, B. Autenrieth, C.K. Weiss, K. Landfester, V. Mailander, The Softer and More Hydrophobic the Better: Influence of the Side Chain of Polymethacrylate Nanoparticles for Cellular Uptake, Macromol Biosci, 10 (2010) 1034-1042.
[17] L.S. Wan, Z.K. Xu, X.J. Huang, Z.G. Wang, P. Ye, Hemocompatibility of poly(acrylonitrile-co-N-vinyl-2-pyrrolidone)s: swelling behavior and water states, Macromol Biosci, 5 (2005) 229-236.
[18] L. Boguslavsky, S. Baruch, S. Margel, Synthesis and characterization of poly acrylonitrile nanoparticles by ispersion/emulsion polymerization process, J Colloid Interf Sci, 289 (2005) 71-85.
[19] T. Biswal, R. Samal, P.K. Sahoo, Co(III) Complex Mediated Microwave-Assisted Synthesis of PAN, J Appl Polym Sci, 117 (2010) 1837-1842.
[20] J.M. Lee, S.J. Kang, S.J. Park, Synthesis of Polyacrylonitrile Based Nanoparticles via Aqueous Dispersion Polymerization, Macromol Res, 17 (2009) 817-820.
[21] K. Landfester, M. Antonietti, The polymerization of acrylonitrile in miniemulsions: "Crumpled latex particles" or polymer nanocrystals, Macromol Rapid Comm, 21 (2000) 820-824.
[22] W.K. Oh, Y.S. Jeong, J. Song, J. Jang, Fluorescent europium-modified polymer nanoparticles for rapid and sensitive anthrax sensors, Biosens Bioelectron, 29 (2011) 172-177.
[23] W. Li, B.F. Pierce, N. Scharnagl, C. Wischke, A. Lendlein, Influence of the co-monomer ratio on teh chemical properties and cytotoxicity of poly[acrylonitrile-*co*-(*N*-vinylpyrrolidone]nanoparticles, J Appl Biomat Funct Mat, 10 (2012) 308-314.
[24] J.A. Alduncin, J. Forcada, M.J. Barandiaran, J.M. Asua, On the Main Locus of Radical Formation in Emulsion Polymerization Initiated by Oil-Soluble Initiators, J Polym Sci Pol Chem, 29 (1991) 1265-1270.
[25] P.J. Blythe, A. Klein, J.A. Phillips, E.D. Sudol, M.S. El-Aasser, Miniemulsion polymerization of styrene using the oil-soluble initiator AMBN, J Polym Sci Pol Chem, 37 (1999) 4449-4457.
[26] C. Hou, C.G. Wang, H.S. Cai, W.X. Zhang, Determination of the reactivity ratios for acrylonitrile/N-vinylpyrrolidone copolymerization systems, J Appl Polym Sci, 89 (2003) 422-425.
[27] L.S. Wan, Z.K. Xu, X.J. Huang, Asymmetric membranes fabricated from poly(acrylonitrile-co-N-vinyl-2-pyrrolidone)s with excellent biocompatibility, J Appl Polym Sci, 102 (2006) 4577-4583.
[28] C.A. Dinarello, Immunological and inflammatory functions of the interleukin-1 family, Annual review of immunology, 27 (2009) 519-550.
[29] V. Mako, J. Czucz, Z. Weiszhar, E. Herczenik, J. Matko, Z. Prohaszka, L. Cervenak, Proinflammatory activation pattern of human umbilical vein endothelial cells induced by IL-1beta, TNF-alpha, and LPS, Cytometry. Part A : the journal of the International Society for Analytical Cytology, 77 (2010) 962-970.